10.24425/acs.2022.141716

Archives of Control Sciences
Volume 32(LXVIII), 2022
No. 2, *pages* 359–381

Pitch and yaw motion control of 2 DoF helicopter subjected to faults using sliding-mode control

M. RAGHAPPRIYA and S. KANTHALAKSHMI

This paper presents a fault-tolerant control scheme for a 2 DOF helicopter. The 2 DOF helicopter is a higher-order multi-input multi-output system featuring non-linearity, cross-coupling, and unstable behaviour. The impact of sensor, actuator, and component faults on such highly complex systems is enormous. This work employs sliding mode control, which is based on reaching and super-twisting laws, to handle the problem of fault control. Simulation tests are carried out to show the effectiveness of the algorithms. Various performance metrics are analyzed and the results show SMC based on super-twisting law provides better control with less chattering. The stability of the closed-loop system is mathematically assured, in the presence of faults, which is a key contribution of this research.

Key words: fault tolerant control, sliding mode control, reaching law, super-twisting, sensor, actuator and component faults

1. Introduction

With the growing use of helicopters in civic and industrial applications such as transportation, air-sea rescue, firefighting, military, and surveillance, key concerns such as safety and reliability are becoming increasingly important. Helicopters are nonlinear by nature, with intrinsic unstability, cross-coupling effects, unmodeled dynamics, and parametric uncertainties. Its versatility originates from its unique maneuvering characteristics, which include the ability to fly long distances at low altitudes, take off and land quickly, fly at low speeds with excellent stability, and hover throughout operations to meet specific needs. Furthermore, the flight control issue is loaded with complexities. Flight stability can be dis-

M. Raghappriya is with Department of Electronics and Instrumentation Engineering, Government College of Technology, Coimbatore, India.

S. Kanthalakshmi is with Department of Electrical and Electronics Engineering, PSG College of Technology, Coimbatore, India.

Received 8.10.2021. Revised 9.2.2022.

rupted by altitude, load, environmental conditions, complex systems, nonlinear aerodynamics, and changes in flight conditions. Various sensors, measurement systems, and actuation systems are integrated into these systems to make them completely functional. These measurement systems are susceptible to faults and uncertainties, resulting in decreased system performance, safety, and reliability. Faults in measurement and actuation systems can have disastrous implications if they are not addressed effectively [11, 12].

To solve stability concerns and improve system performance in the face of faults and uncertainties, a Fault-Tolerant Controller (FTC) must be designed [2, 4, 21]. A fault-tolerant controller is a control system that can ensure system safety in the event of faults occurring in the system while performing regular control functions [19]. Numerous research works have been carried out in the field of FTC for aerial systems [20]. In the presence of uncertainty, Sliding Mode Control (SMC) is one of the most effective strategies [3]. SMC improves the system's robustness and compensates for changes in parameters. It is not reliant on a precise mathematical model and can accurately track the reference model. The following researches highlights the various structures of sliding mode control for a 2 degrees of freedom (DOF) helicopter.

A robust control technique using sliding mode control based on tracking from external disturbance observer is designed in [17] for a linear model of helicopter. A fault-tolerant adaptive sliding mode control method for a multirotor helicopter is discussed in [18]. The virtual control part and the control allocation part together makes up the control structure. The control allocation part distributes virtual control signals to fault-free and faulty actuators for minor actuator faults. When multiple faults occur simultaneously, the adaptive method is activated to compensate for the virtual control signal generated by the control allocation component. An adaptive FTC method for non-linear MIMO systems with uncertainties subjected to actuator faults is presented in [10]. This method uses sliding mode control and the actuator fault is represented as a loss of effectiveness. The fault is modeled as multiplicative factor of control signal. The method is simulated for 2 DOF helicopter and robotic manipulator system. [7] developed an augmented sliding mode control for tracking control in Quadrotor Unmanned Aerial Vehicles (QAV) under propeller damage and actuator fault conditions. The developed controller is built using two FTC methodologies, both passive and active, and the benefits and drawbacks are compared with and without faults.For a 3 DOF helicopter system with actuator drift and oscillation faults as well as saturation, a fault estimation based FTC is devised in [6]. The actuator faults are integrated into the system as a non-differentiable fault function and the system states are estimated using unknown input observer. Based on estimated states, an adaptive sliding mode controller is designed to mitigate the effects of actuator faults. A neural network based classification method and a fuzzy based control method is designed in [15] for 2 DOF helicopter with different types of

actuator faults. A nonsingular terminal sliding mode control based passive FTC is explored in [14] for a 3 DOF helicopter system. The FTC presented takes care of actuator failure in pitch and yaw motors. The challenge of trajectory tracking for a quadrotor unmanned aerial vehicle experiencing simultaneous actuator faults, external disturbances, and actuator saturation limitations is addressed in [8] using an observer-based robust adaptive fault tolerant control technique. The unmeasured states are estimated using a fuzzy state observer. An integral sliding mode control is designed based on estimated states.

A robust anti swing tolerant control scheme is developed in [9] for an unmanned helicopter with sensor faults. A sensor fault estimator is designed based on the non-linear motion model of helicopter and the estimated states are used for the design of robust control based on sliding mode control and back stepping technique. An non-linear FTC for hypersonic vehicle with multisensor faults is presented in [1]. To diagnose sensor faults, a backstepping adaptive sliding mode observer is utilized, and the estimation findings are used to construct a non-linear FTC to compensate for multi-sensor faults. [13] proposed an active fault-tolerant control scheme for a quadrotor with velocity sensor faults. External-loop Proportion Differentiation (PD) control law and internal-loop Proportion Integration Differentiation (PID) control law are used in a two-level control scheme. Using a Luenberger observer-based residual generator, fault detection is accomplished. A fault-tolerant control law is developed by integrating the external-loop PD control law with the outcome of fault estimation. Based on robust integral backstepping approach using sliding mode [5], the control strategy is formed for a quadrotor system in the presence of sensor faults. [16] examines the sliding mode fault-tolerant control of an unmanned aerial vehicle, taking into account sensor and actuator failures. The parameters of the SMC are designed using RBF neural network algorithm. The faults dealt includes faults in accelerometer sensor, gyroscope sensor and actuators.

The motivation behind this work is to design FTC based control for a 2 DOF helicopter system in the presence of faults and parameter uncertainties. Among the faults affecting the system, besides sensor and actuator faults, component faults are also considered. To mitigate the effects of faults, two variants of sliding mode control are designed and their performance is compared. The major contribution of this work is highlighted below.

- Design of reaching law SMC and super twisting SMC for a non-linear 2 DOF helicopter system.
- The control scheme designed can tolerate three different types of faults i.e., sensor, actuator, and component faults represented as additive and multiplicative models.
- Performance analysis is made between reaching law SMC and super twisting SMC based on the simulated results.

- Lyapunov-based stability analysis is carried out to ensure the stability of the helicopter system with FTC control.

2. Preliminaries

2.1. 2 DOF helicopter modeling

The 2 degrees of freedom in the helicopter are the pitch angle and yaw angle. Figure 1 shows the schematic of 2 DOF helicopter. The setup comprises a body, two propellers, two DC motors and two encoders for the helicopter pitch and yaw angles. A permanent base platform supports the helicopter body attached to the yoke. The front propeller, which controls the altitude of the helicopter nose around the pitch axis, is driven by the pitch DC motor. The back propeller is controlled by the yaw DC motor, which controls the horizontal motions of the helicopter around the yaw axis. Pitch and yaw encoders are used to measure the true pitch and yaw angles of a helicopter, respectively.

Figure 1: 2 DOF helicopter

The free body diagram of 2 DOF helicopter is shown in Fig. 2. F_p and F_y are thrust forces exerted across the pitch and yaw axis, respectively. r_p and r_y are the distances at which the torque acts from the respective axis. F_g is the gravitational

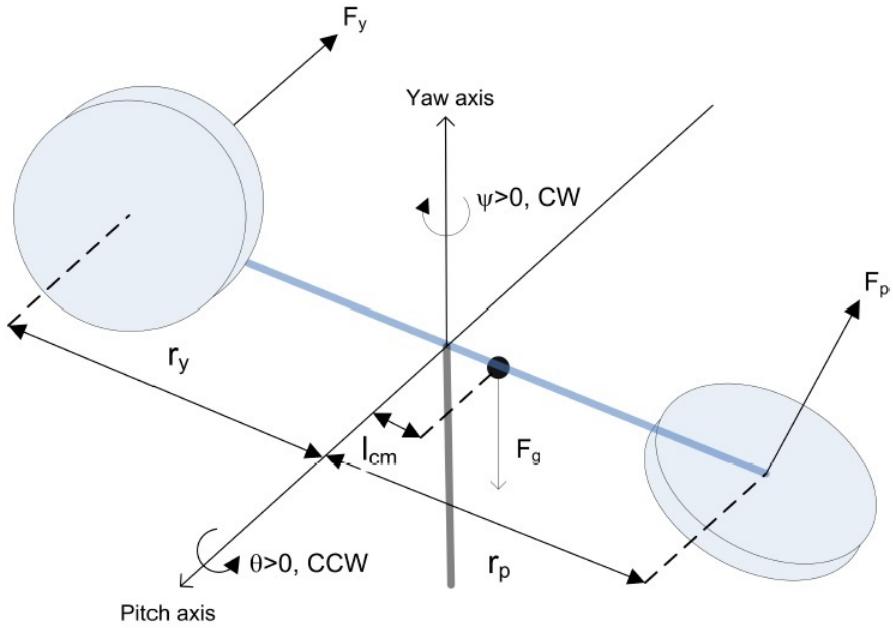

Figure 2: Free body diagram of 2 DOF helicopter

force and l_{cm} is the distance at which the centre of mass acts from the helicopter body. The Euler's-Lagrange equation is used to derive the non-linear motion model of the helicopter system. The Lagrangian is

$$L = T - V, \tag{1}$$

where T is the total kinetic energy and V is the total potential energy.

The total kinetic energy is given by

$$T = \frac{1}{2} J_{eq,p} \dot{\theta}^2 + \frac{1}{2} J_{eq,y} \dot{\psi}^2 + \frac{1}{2} m_{\text{heli}} l_{cm}^2 \left[\dot{\theta}^2 + \dot{\psi}^2 \cos^2 \theta \right]. \tag{2}$$

The total potential energy due to gravity is given by

$$V = m_{\text{heli}} g \sin \theta l_{cm}. \tag{3}$$

Non-linear dynamics are captured using generalized coordinates that describe the system behaviour. Thus the Euler-Lagrange equation is written as

$$\left[\frac{\partial^2}{\partial t \partial n} L \right] - \left[\frac{\partial}{\partial n} L \right] = Q_n, \qquad n \in [\theta, \psi], \tag{4}$$

Table 1: Nominal parameters of helicopter

Symbol	Description	Value	Unit
K_{pp}	Thrust force constant of yaw propeller	0.204	N · m/V
K_{py}	Thrust torque constant of pitch axis from yaw propeller	0.0068	N · m/V
K_{yp}	Thrust torque constant of yaw axis from pitch propeller	0.0219	N · m/V
K_{yy}	Thrust torque constant of yaw axis from yaw propeller	0.0072	N · m/V
B_p	Equivalent viscous damping about pitch axis	0.800	N/V
B_y	Equivalent viscous damping about yaw axis	0.318	N/V
m_{heli}	Total moving mass of the helicopter	1.3872	Kg
l_{cm}	Center of mass length along helicopter body from pitch axis	0.186	mv
$J_{eq,p}$	Total moment of inertia about pitch axis	0.0384	$Kg \cdot m^2$
$J_{eq,y}$	Total moment of inertia about yaw axis	0.0432	$\text{Kg} \cdot \text{m}^2$
$V_{m,p}$	Pitch motor voltage	± 24	V
$V_{m,y}$	Yaw motor voltage	± 15	V

Q_θ and Q_ψ are the generalized forces corresponding to generalized coordinates. Based on the torque acting on pitch and yaw axis, Q_θ and Q_ψ becomes

$$Q_\theta = K_{pp}V_{m,p} + K_{py}V_{m,y} - B_p\dot{\theta}\,, \tag{5}$$

$$Q_\psi = K_{yp}V_{m,p} + K_{yy}V_{m,y} - B_y\dot{\psi}\,. \tag{6}$$

Substituting equation (1), (2) and (3) into equation (4), the nonlinear equations of motion of the helicopter system is derived as

$$\begin{aligned}(J_{eq,p} + m_{\text{heli}}l_{cm}^2)\ddot{\theta} = {} & K_{pp}V_{m,p} + K_{py}V_{m,y} - B_p\dot{\theta} - m_{\text{heli}}gl_{cm}\cos\theta \\ & - m_{\text{heli}}l_{cm}^2\sin\theta\cos\theta\dot{\psi}^2,\end{aligned} \tag{7}$$

$$\begin{aligned}(J_{eq,y} + m_{\text{heli}}l_{cm}^2\cos^2\theta)\ddot{\psi} = {} & K_{yp}V_{m,p} + K_{yy}V_{m,y} - B_y\dot{\psi} \\ & + 2m_{\text{heli}}l_{cm}^2\sin\theta\cos\theta\dot{\theta}\dot{\psi}.\end{aligned} \tag{8}$$

The above equations are modified for simplification as

$$J_\theta\ddot{\theta} = K_{pp}V_{m,p} + K_{py}V_{m,y} - q_\theta\,, \tag{9}$$

$$J_\psi\ddot{\psi} = K_{yp}V_{m,p} + K_{yy}V_{m,y} - q_\psi\,, \tag{10}$$

with the following notations defined as

$$J_\theta = J_{eq,p} + m_{\text{heli}}l_{cm}^2\,, \tag{11}$$

$$J_\psi = J_{eq,y} + m_{\text{heli}} l_{cm}^2 cos^2\theta\,, \tag{12}$$

$$q_\theta = B_p\dot{\theta} + m_{\text{heli}} g l_{cm}\cos\theta + m_{\text{heli}} l_{cm}^2 \sin\theta\cos\theta\dot{\psi}^2, \tag{13}$$

$$q_\psi = B_y\dot{\psi} - 2m_{\text{heli}} l_{cm}^2 \sin\theta\cos\theta\dot{\theta}\dot{\psi}\,. \tag{14}$$

The non-linear state space model has the form $\dot{x} = f(x) + g(x,u)$. By considering the position and velocity coordinates, the nonlinear state-space model of the helicopter is framed as

$$\underbrace{\begin{bmatrix}\dot{\theta}\\ \dot{\psi}\\ \ddot{\theta}\\ \ddot{\psi}\end{bmatrix}}_{\dot{x}} = \underbrace{\begin{bmatrix}\dot{\theta}\\ \dot{\psi}\\ \frac{1}{J_\theta}[-q_\theta + w]\\ \frac{1}{J_\psi}[-q_\psi + w]\end{bmatrix}}_{f(x)} + \underbrace{\begin{bmatrix}0 & 0\\ 0 & 0\\ \frac{K_{pp}}{J_\theta} & \frac{K_{py}}{J_\theta}\\ \frac{K_{yp}}{J_\psi} & \frac{K_{yy}}{J_\psi}\end{bmatrix}\begin{bmatrix}V_{m,p}\\ V_{m,y}\end{bmatrix}}_{g(x,u)}\,. \tag{15}$$

The state vectors are pitch angle θ, yaw angle ψ, pitch velocity $\dot{\theta}$, and yaw velocity $\dot{\psi}$. Thus $X = [\theta\ \psi\ \dot{\theta}\ \dot{\psi}]^T$. Pitch motor voltage $V_{m,p}$ and Yaw motor voltage $V_{m,y}$ are the two inputs u_θ, u_ψ to the helicopter. The two measured outputs are the pitch angle and yaw angle. The output vector is given by

$$y = [\theta\ \psi]^T + v. \tag{16}$$

The model is augmented with two lumped disturbance factors w and v, to address the problem of parametric uncertainties and unknown disturbances. Wind effects, atmospheric turbulence, gyroscopic torques, and couplings induced by the front and rear propellers are some of the unmodeled variables and disturbances affecting the system.

2.2. 2 DOF helicopter fault modeling

Sensor faults, actuator faults and component faults are the faults which are predominantly affecting the helicopter. For control and stabilization of helicopter, precise location and attitude data are required from the sensors. Sensors in autonomous helicopters can malfunction in a variety of ways. Gain reduction or loss of precision, persistent offset or bias, sensor drift or frozen sensor are all types of sensor faults.

Out of all the sensor faults mentioned, this paper deals with the sensor drift which occurs mostly due to temperature changes or any changes in the calibration of sensor. Drift is modeled as a vector b_j that affects the system measurements. Pitch and yaw angle, which are measured by pitch and yaw encoders, are the

helicopter outputs. Thus, the system output with the presence of sensor fault gets changed as

$$y = [\theta \ \psi]^T + b_j, \forall j = 1, 2, ...n, \tag{17}$$

where n denotes the number of sensors. Here b_j is a column vector.

Actuators are critical components of the helicopter system because they provide a link between control commands and physical activity. A failure of an actuator in a helicopter can be harmful since it might cause the helicopter to lose control and crash. Actuator faults can occur as a result of float failure, lock failure, hard over faults, or partial faults such as hydraulic leakage, supply voltage change, or a stuck actuator owing to a lack of lubrication. The type of actuator fault dealt in this paper is loss of control effectiveness of actuator. The loss of control effectiveness of actuators is denoted by a factor l_k where k denotes the number of actuators. Thus, actuator fault for pitch and yaw propeller is modeled as

$$u_f = \text{diag}[1 - l_1 \ \ 1 - l_2][u_\theta \ u_\psi]^T. \tag{18}$$

Component faults are primarily defined as changes in the physical parameters of the system, such as mass, aerodynamic coefficient, centre of gravity, or damping constant. A change in the parameter of the system state equation is considered as component fault. This is denoted as Δx.

2.3. Problem formulation

Consider a nonlinear helicopter system with model uncertainties and faults as

$$\dot{x}(t) = f(x(t), \Delta x(t), b_j, t) + g(u(t), l_k) + d(t), \tag{19}$$

where $x(t)$ is the state vector, $u(t)$ is the control input, and f is the nonlinear function. $d(t)$ implies the bounded unknown disturbances acting on the system. b_j is the vector representing the sensor bias fault where the magnitude of bias b_j is $0 \leqslant b_j \leqslant 1$. The loss of control effectiveness of actuator is represented as l_k where k denotes the number of actuators. l_k satisfies $0 \leqslant l_k \leqslant 1$ with the fault free case of actuator indicated with the value $l_k = 0$ and the complete failure has l_k value as 1. $\Delta x(t)$ denotes the change in the system state due to change in system parameters. The generic model denoted represents the system with sensors, actuator and component faults.

3. Controller design

The overall FTC strategy is depected in Fig. 3. r_i denotes the system setpoint. In a traditional SMC design, there are usually two phases. The first step entails creating a sliding surface that ensures the desired system tracking performance.

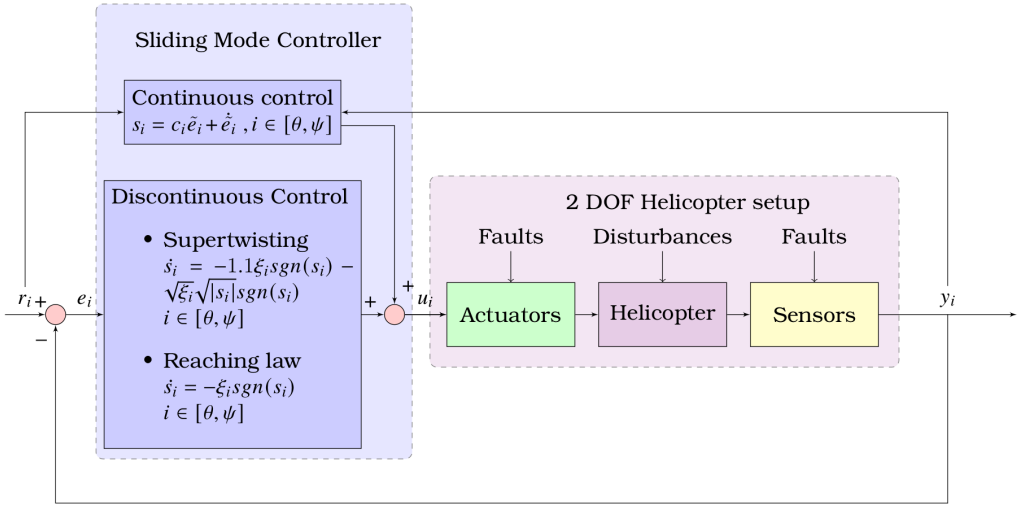

Figure 3: FTC Strategy for 2 DOF Helicopter

The second step entails selecting a suitable control strategy for driving the relevant sliding variable onto the proposed sliding surface and then maintaining the sliding motion within a close proximity to the sliding surface. Let θ_d and ψ_d represents the desired system trajectory of pitch and yaw angle respectively. The tracking error is given by

$$\tilde{e} = [e_\theta \;\; e_\psi]^T = [\theta_d - \theta \;\; \psi_d - \psi]^T. \tag{20}$$

The sliding surface for accurate tracking of the pitch and yaw angle is chosen as $s = [s_\theta \;\; s_\psi]^T$ with

$$s_i = c_i\tilde{e}_i + \dot{\tilde{e}}_i\,, \qquad i \in [\theta, \psi], \tag{21}$$

where c_i is the coefficient of Hurwitz polynomial. c_i should be chosen strictly positive which ensures that the closed loop system is asymptotically stable during the ideal sliding mode.

To investigate the sliding motion associated with the sliding function, compute the time derivative as follows.

$$\dot{s}_i = c_i\dot{\tilde{e}}_i + \ddot{\tilde{e}}_i\,, \qquad i \in [\theta, \psi], \tag{22}$$

$$\dot{s}_i = \begin{cases} \dot{s}_\theta \\ \dot{s}_\psi \end{cases} = \begin{cases} c_\theta \dot{e_\theta} + \ddot{\theta}_d - \ddot{\theta} \\ c_\psi \dot{e_\psi} + \ddot{\psi}_d - \ddot{\psi} \end{cases} \tag{23}$$

After choosing the sliding surface, the challenge is to come up with an appropriate control law that will make the sliding surface desirable.

There are two parts in the control law: continuous control and discontinuous control. The continuous control which stabilizes the ideal system is designed by making $\dot{s}_i = 0$.

$$c_i \dot{\tilde{e}}_i + \ddot{\tilde{e}}_i = 0. \tag{24}$$

However, the helicopter is bound to be affected by external disturbances $d(t)$ which is modeled as w and v. Thus error dynamics will now become

$$c_i \dot{\tilde{e}}_i + \ddot{\tilde{e}}_i = d(t). \tag{25}$$

As a result of these external disturbances, the tracking error and derivative will not converge to zero. Thus to compensate for these external disturbances and to retain desired sliding motion, a discontinuous control is designed.

3.1. Reaching law SMC based FTC

A sliding surface $s = 0$ design with relative degree one with respect to the control makes up the first order sliding mode control. Convergence occurs in finite time after the states reach the surface. The discontinuous control signal using constant rate reaching law is given by

$$\dot{s}_i = -\xi_i \operatorname{sgn}(s_i), \qquad i \in [\theta, \psi], \tag{26}$$

where ξ is the constant rate and sgn is the signum function. The value of ξ determines the switching heights and chattering. Thus combining the continuous and discontinuous control, the control signals to be fed to the helicopter are determined as

$$\begin{aligned} V_{m,p} = K_1 \Big[& K_{yy} J_\theta [c_\theta \dot{e}_\theta + \ddot{\theta}_d + \xi_\theta \operatorname{sgn}(s_\theta)] + K_{yy} q_\theta \\ & - K_{py} J_\psi [c_\psi \dot{e}_\psi + \ddot{\psi}_d + \xi_\psi \operatorname{sgn}(s_\psi)] - K_{py} q_\psi \Big], \end{aligned} \tag{27}$$

$$\begin{aligned} V_{m,y} = -K_1 \Big[& K_{yp} J_\theta [c_\theta \dot{e}_\theta + \ddot{\theta}_d + \xi_\theta \operatorname{sgn}(s_\theta)] + K_{yp} q_\theta \\ & - K_{pp} J_\psi [c_\psi \dot{e}_\psi + \ddot{\psi}_d + \xi_\psi \operatorname{sgn}(s_\psi)] - K_{pp} q_\psi \Big] \end{aligned} \tag{28}$$

with

$$K_1 = \frac{1}{K_{pp} K_{yy} - K_{py} K_{yp}}. \tag{29}$$

The chattering phenomenon, which is characterised by tiny oscillations at the system's output, is the primary disadvantage of the conventional sliding mode. System's rapid dynamics and discontinuity in the control signal are the major causes of chattering.

3.2. Supertwisting SMC based FTC

Another second-order sliding mode control termed super twisting control is used to reduce the chattering phenomenon inherent in reaching law. In second order sliding mode control, the second derivative of the sliding variable is used. It provides for the convergence to zero of both the sliding variable and its derivative in finite time. Through a continuous control acting discontinuously on the sliding variable's second time derivative, the super twisting method zeros the sliding variable and its first time derivative in a finite time thereby reducing chattering. The control method is robust to the effect of parameter uncertainties. The control technique is also impervious to disturbance and noise because it does not require derivative feedback of the sliding variable. The system states can be made to approach the equilibrium point in a finite amount of time using super-twisting sliding mode control. The super twisting discontinuous control which eliminates chattering while preserving robustness is given by

$$\dot{s}_i = -1.1\xi_i \text{sgn}(s_i) - \sqrt{\xi_i}\sqrt{|s_i|}\text{sgn}(s_i)\ , i \in [\theta, \psi] \tag{30}$$

From the equations, the pitch and yaw control signal from super twisting control is

$$\begin{aligned} V_{m,p} = K_1 \Big[& K_{yy} J_\theta \Big[c_\theta \dot{e}_\theta + \ddot{\theta}_d + 1.1\xi_\theta \text{sgn}(s_\theta) + \sqrt{\xi_\theta}\sqrt{|s_\theta|}\text{sgn}(s_\theta) \Big] \\ & + K_{yy} q_\theta - K_{py} J_\psi \Big[(c_\psi \dot{e}_\psi + \ddot{\psi}_d + 1.1\xi_\psi \text{sgn}(s_\psi) \\ & + \sqrt{\xi_\psi}\sqrt{|s_\psi|}\text{sgn}(s_\psi) \Big] - K_{py} q_\psi \Big] \end{aligned} \tag{31}$$

$$\begin{aligned} V_{m,y} = -K_1 \Big[& K_{yp} J_\theta \Big[c_\theta \dot{e}_\theta + \ddot{\theta}_d + 1.1\xi_\theta \text{sgn}(s_\theta) + \sqrt{\xi_\theta}\sqrt{|s_\theta|}\text{sgn}(s_\theta) \Big] \\ & + K_{yp} q_\theta - K_{pp} J_\psi \Big[c_\psi \dot{e}_\psi + \ddot{\psi}_d + 1.1\xi_\psi \text{sgn}(s_\psi) \\ & + \sqrt{\xi_\psi}\sqrt{|s_\psi|}\text{sgn}(s_\psi) \Big] - K_{pp} q_\psi \Big]. \end{aligned} \tag{32}$$

4. Results and discussions

In this section, simulation results are presented to demonstrate the effectiveness of the FTC strategies presented in the previous section. The helicopter's original position is presumed to be at origin. The system is sampled every 0.005 seconds and simulated for 10000-time instants. Focusing on the faults occurring in the system, three different faults are tested. These faults are added as additive and multiplicative faults. Multiplicative faults frequently mix with system states and/or inputs, whereas additive faults usually appear as offsets. Regardless of

faults, the goal of the control is to keep the system outputs at the desired value. The results indicate how controllers operate when sensor, actuator, and component faults occur. In addition, various performance metrics like Integral Square Error (ISE), Integral Absolute Error (IAE), Integral Time Square Error (ITSE), and Integral Time Absolute Error (ITAE) are calculated in order to statistically analyse the control performance.

4.1. Sensor fault

Pitch and yaw encoders, which operate as sensors in the system, are used to measure helicopter outputs. Sensor bias, which impacts the system outputs, is the fault being investigated. The magnitude of bias vector b_j varies between $0 \leqslant b_j \leqslant 1$. b_1 and b_2 denotes bias in sensor 1 and 2. Here two scenarios are considered. In Scenario 1, a 20% bias ($b_j = 0.2$) in pitch and yaw encoder is introduced at $t = 5000$ as an additive fault. At $t = 5000$, Scenario 2 introduces a multiplicative fault of 20% bias ($b_j = 0.2$) in pitch and yaw encoders.

The motion tracking performance of helicopter under scenario 1 is demonstrated in Fig. 4. The desired position r_i is chosen as $[\theta \ \ \psi]^T = [1 \ \ 2]^T$. As seen,

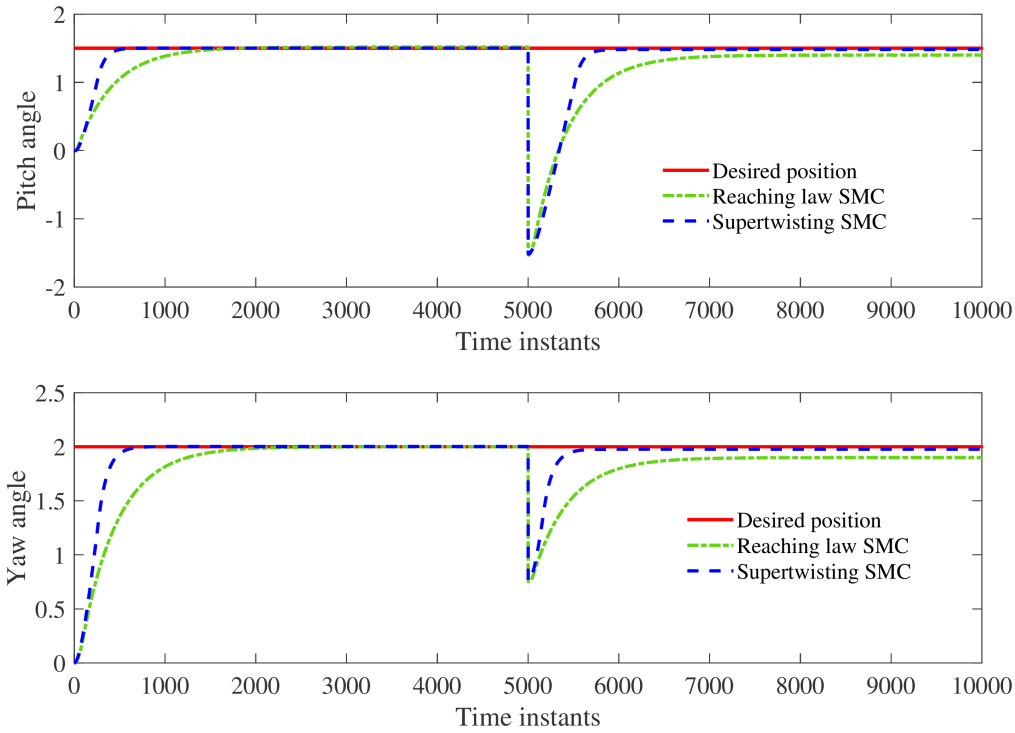

Figure 4: System outputs with additive sensor fault

the system is disrupted from its desired position after a fault occurs. To offset the fault, both controllers boost the control input to the helicopter and strive for original tracking performance. Supertwisting FTC outperforms reaching law FTC in terms of tracking performance. In terms of control effort, it is evident from Fig. 5, chattering is significantly reduced in supertwisting control when the sensor fault occurs.

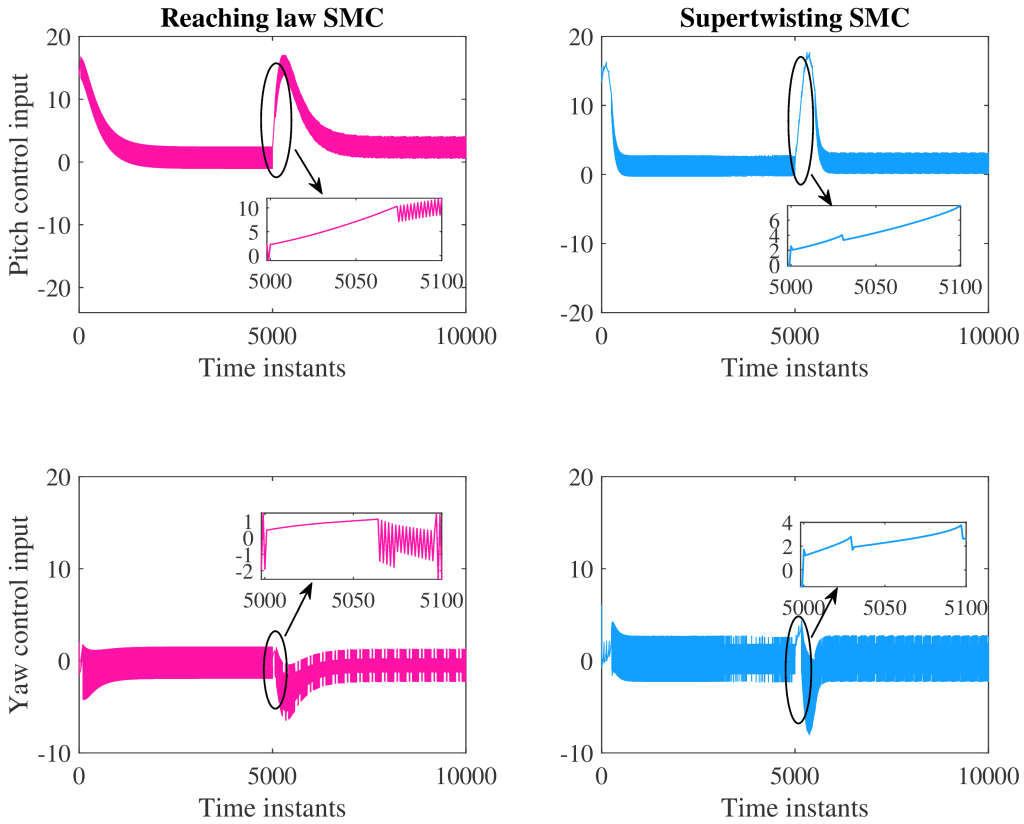

Figure 5: Controller action for additive sensor fault

In scenario 2, the bias in sensor is introduced as multiplicative fault. The multiplicative character of faults has a greater impact on system outputs. The variation of pitch and yaw angles, as well as the control effort necessary to keep the system in the desired position, are shown in Fig. 6.

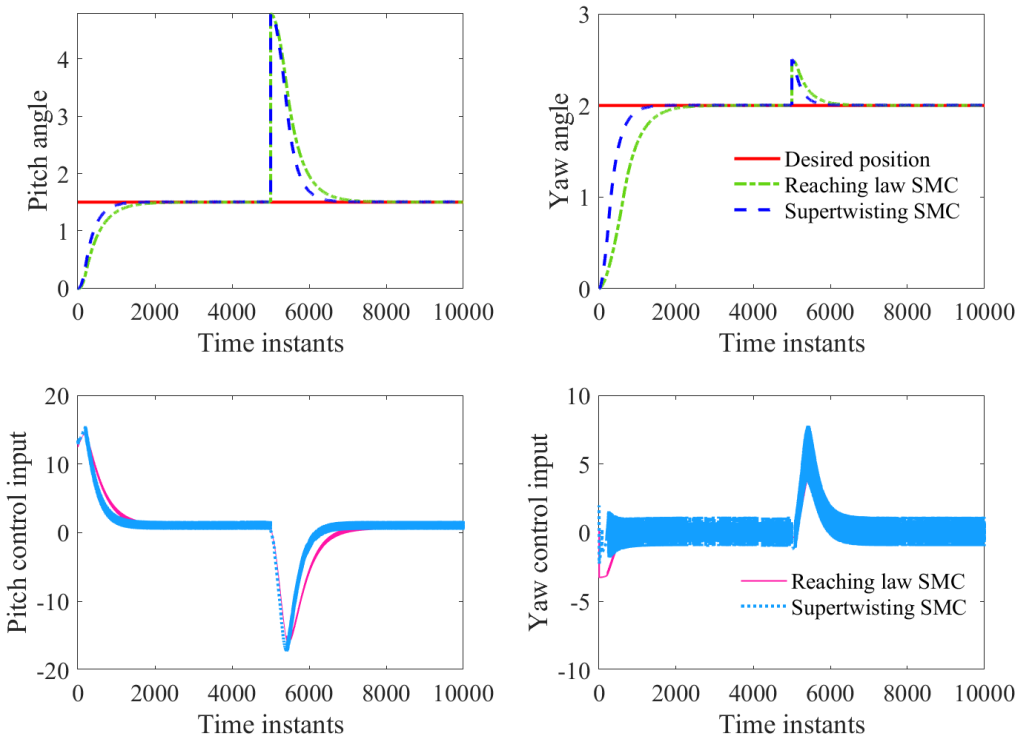

Figure 6: Helicopter outputs and controller signal for multiplicative sensor fault

4.2. Actuator fault

The actuators in the helicopter system are the pitch and yaw propellers, driven by pitch and yaw motor respectively. The control signals fed to these actuators are the voltage signals required to drive these motors. Thus actuator fault is represented as loss in control effectiveness of actuators. The magnitude of loss in control effectiveness is chosen as $l_1 = 0.3$ and $l_2 = 0.3$. Thus faulty control signal u_f is introduced into the system at $t = 5000$. Again two scenarios are presented.

In scenario 1, u_f is given as an additive signal. The output for scenario 1 is depicted in Fig. 7. Once the fault occurs, a large deviation from the original position is witnessed and the controllers attempt to bring the outputs back to their original position. The Fig. 7 also depicts the control effort put in by both controllers, where large chattering is encountered by the fault control developed from reaching law.

The faulty input signal u_f is injected as a multiplicative fault in scenario 2. Fig. 8 and Fig. 9 represents the helicopter states and the control effort generated by 2 controllers for the actuator fault. Again the supertwisting controller portrays better performance and minimum chattering.

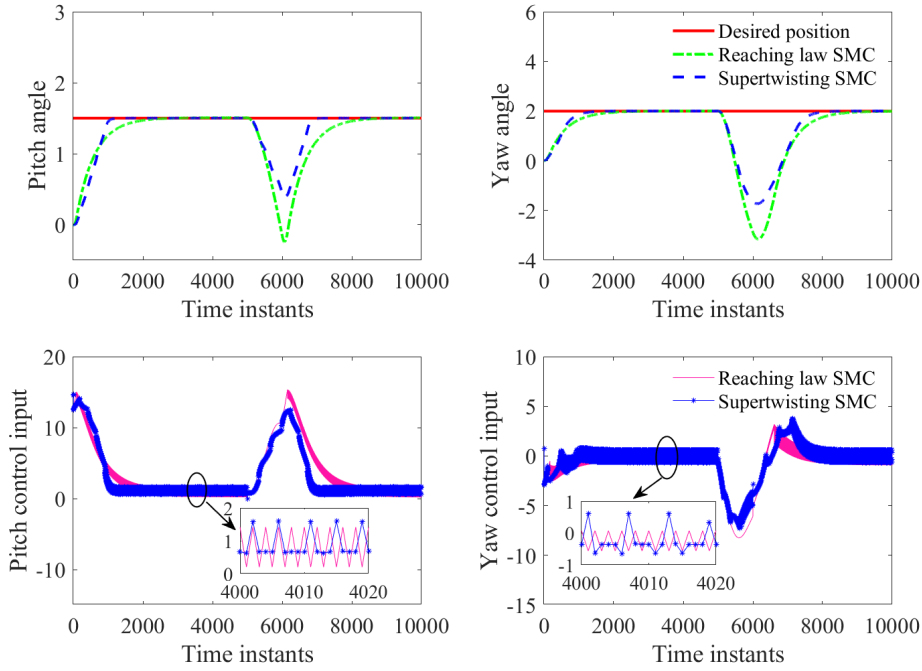

Figure 7: Helicoptor output and control signal for additive actuator fault

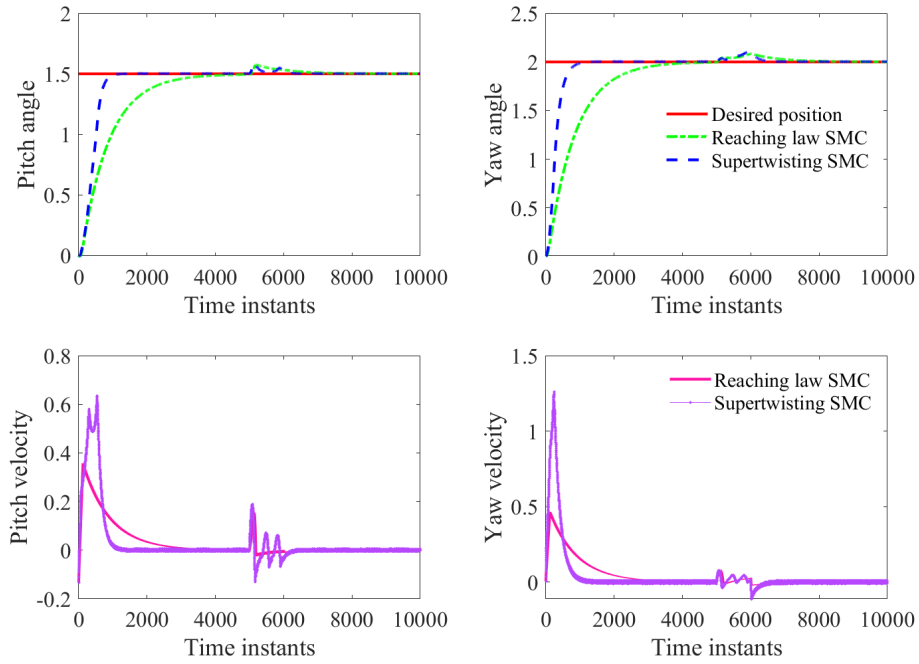

Figure 8: Helicoptor states for multiplicative actuator fault

Table 2: Performance metrics of 2 DOF Helicopter

Controller type	Fault model	Fault type	ISE		IAE		ITSE		ITAE	
			θ	ψ	θ	ψ	θ	ψ	θ	ψ
Supertwisting SMC	Additive	Sensor	$2.56 \cdot 10^3$	852.40	$1.43 \cdot 10^3$	810.60	$1.15 \cdot 10^7$	$1.10 \cdot 10^6$	$6.06 \cdot 10^6$	$2.11 \cdot 10^6$
		Actuator	$1.67 \cdot 10^3$	$1.59 \cdot 10^4$	$1.84 \cdot 10^3$	$6.29 \cdot 10^3$	$4.91 \cdot 10^6$	$9.03 \cdot 10^7$	$6.36 \cdot 10^6$	$3.33 \cdot 10^7$
		Component	$2.09 \cdot 10^3$	681.72	$1.45 \cdot 10^3$	729.62	$9.03 \cdot 10^6$	$1.36 \cdot 10^5$	$5.62 \cdot 10^6$	$8.15 \cdot 10^5$
	Multiplicative	Sensor	$4.06 \cdot 10^3$	990.42	$2.17 \cdot 10^3$	895.56	$1.84 \cdot 10^7$	$3.39 \cdot 10^5$	$8.73 \cdot 10^6$	$1.03 \cdot 10^6$
		Actuator	690.27	798.31	687.16	695.30	$1.42 \cdot 10^5$	$1.33 \cdot 10^5$	$4.81 \cdot 10^5$	$6.96 \cdot 10^5$
		Component	$6.17 \cdot 10^3$	$1.41 \cdot 10^3$	$4.27 \cdot 10^3$	$1.86 \cdot 10^3$	$3.23 \cdot 10^7$	$4.27 \cdot 10^6$	$2.27 \cdot 10^7$	$7.69 \cdot 10^6$
Reaching law SMC	Additive	Sensor	$2.84 \cdot 10^3$	$1.44 \cdot 10^3$	$2.44 \cdot 10^3$	$1.89 \cdot 10^3$	$1.25 \cdot 10^7$	$2.73 \cdot 10^6$	$1.10 \cdot 10^7$	$6.82 \cdot 10^6$
		Actuator	$2.48 \cdot 10^3$	$2.55 \cdot 10^4$	$2.58 \cdot 10^3$	$8.11 \cdot 10^3$	$1.10 \cdot 10^7$	$1.50 \cdot 10^8$	$1.11 \cdot 10^7$	$4.42 \cdot 10^7$
		Component	$3.57 \cdot 10^3$	890.19	$2.62 \cdot 10^3$	$1.01 \cdot 10^3$	$1.57 \cdot 10^7$	$2.33 \cdot 10^5$	$1.04 \cdot 10^7$	$1.35 \cdot 10^6$
	Multiplicative	Sensor	$4.92 \cdot 10^3$	$1.97 \cdot 10^3$	$2.77 \cdot 10^3$	$1.62 \cdot 10^3$	$2.22 \cdot 10^7$	$9.08 \cdot 10^5$	$1.11 \cdot 10^7$	$1.79 \cdot 10^6$
		Actuator	$1.09 \cdot 10^3$	$1.83 \cdot 10^3$	$1.40 \cdot 10^3$	$1.83 \cdot 10^3$	$4.60 \cdot 10^5$	$7.70 \cdot 10^5$	$1.51 \cdot 10^6$	$2.10 \cdot 10^6$
		Component	$6.94 \cdot 10^3$	$1.98 \cdot 10^3$	$4.99 \cdot 10^3$	$2.55 \cdot 10^3$	$4.09 \cdot 10^7$	$5.99 \cdot 10^6$	$3.07 \cdot 10^7$	$1.08 \cdot 10^7$

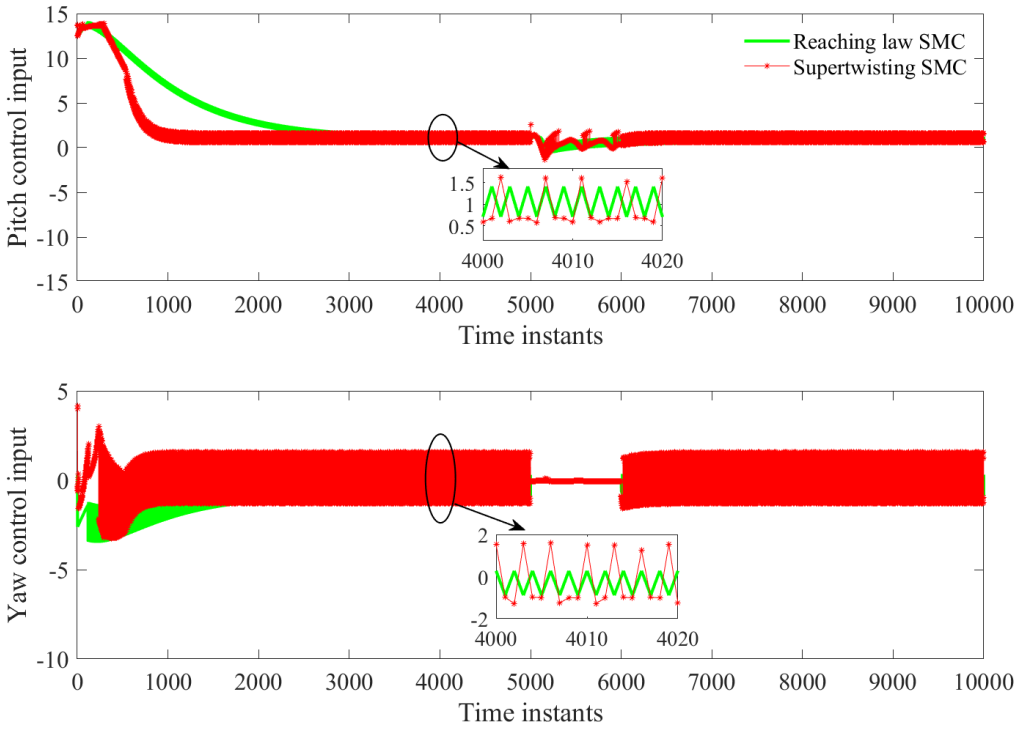

Figure 9: Controller output for multiplicative actuator fault

4.3. Component fault

Change in equivalent viscous damping about the pitch and yaw axis of helicopter is considered as component fault. Thus viscous damping becomes $B_p = 0.5B_p$ and $B_y = 0.5B_y$ from the nominal value at $t = 5000$. Multiplicative fault tends to be more disruptive than the additive component fault as seen from Fig. 10 and Fig. 11. Multiplicative faults produces overshoots and takes larger time to settle. Also the controller action as shown in Fig. 12 is more prone to chattering for component fault.

4.4. Stability analysis

Consider a quadratic Lyapunov function,

$$V = \frac{1}{2}\left(s_\theta^2 + s_\psi^2\right). \tag{33}$$

The Lyapunov function's derivative is calculated as

$$\dot{V} = s_\theta \dot{s_\theta} + s_\psi \dot{s_\psi}\,. \tag{34}$$

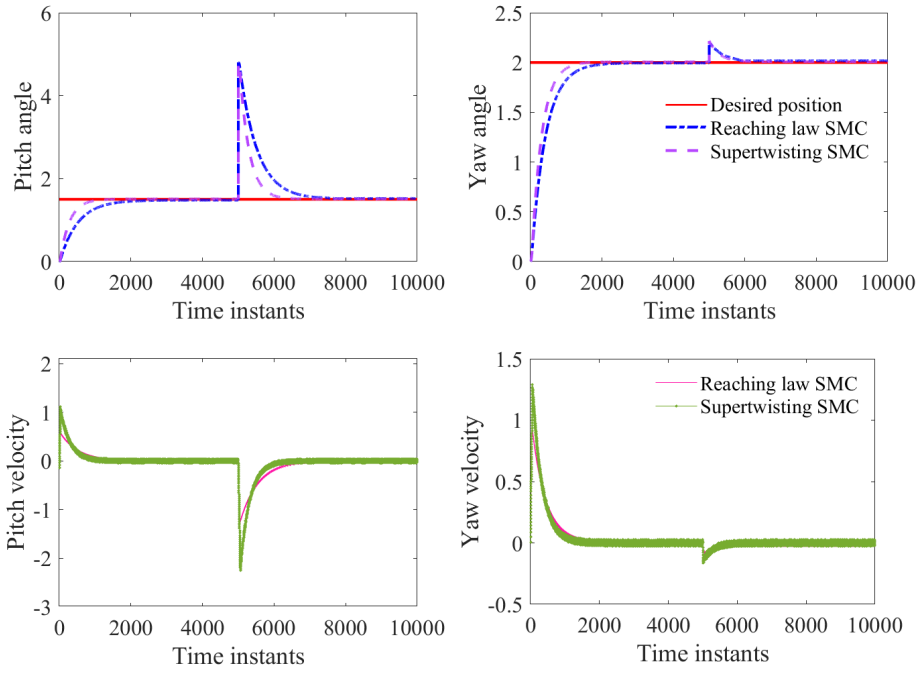

Figure 10: Helicoptor states for additive component fault

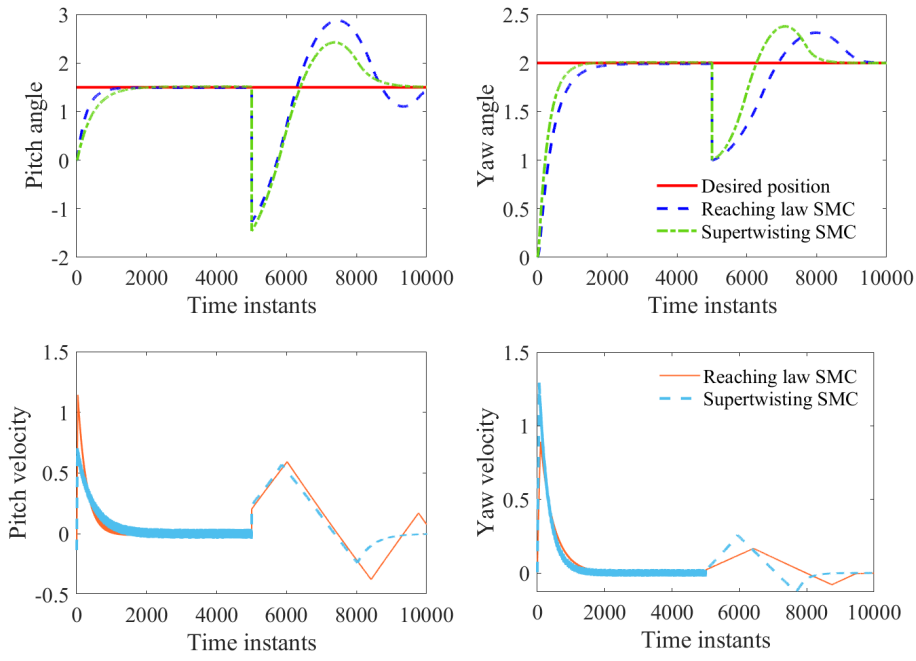

Figure 11: Helicoptor states for multiplicative component fault

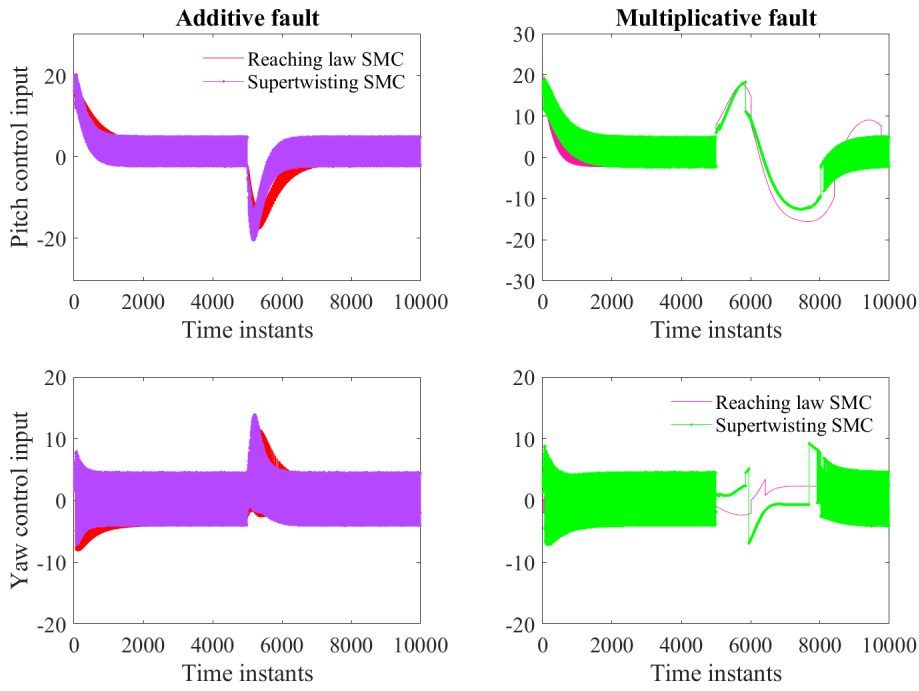

Figure 12: Controller output for component fault

Combining equations (23) and (26), the sliding function for reaching law becomes,

$$\dot{s_\theta} = c_\theta \dot{e_\theta} + \ddot{\theta}_d - \ddot{\theta} + \xi_\theta \text{sgn}(s_\theta), \tag{35}$$

$$\dot{s_\psi} = c_\psi \dot{e_\psi} + \ddot{\psi}_d - \ddot{\psi} + \xi_\psi \text{sgn}(s_\psi) \tag{36}$$

substituting $\ddot{\theta}$ and $\ddot{\psi}$ from system equations (9) and (10)

$$\dot{s_\theta} = c_\theta \dot{e_\theta} + \ddot{\theta}_d + \xi_\theta \text{sgn}(s_\theta) - \frac{K_{pp} V_{m,p} + K_{py} V_{m,y} - q_\theta}{J_\theta}, \tag{37}$$

$$\dot{s_\psi} = c_\psi \dot{e_\psi} + \ddot{\psi}_d + \xi_\psi \text{sgn}(s_\psi) - \frac{K_{yp} V_{m,p} + K_{yy} V_{m,y} - q_\psi}{J_\psi}. \tag{38}$$

Input voltages for pitch and yaw motor $V_{m,p}$ and $V_{m,y}$ is substituted from equations (27) and (28). Thus equation (34) becomes

$$\dot{V} = -s_\theta(\xi_\theta |s_\theta|) - s_\psi(\xi_\psi |s_\psi|), \tag{39}$$

ξ_θ and ξ_ψ is chosen as positive constants which satisfies that the Lyapuvov function becomes negative definite. Following the similar steps, the lyapunov function for

supertwisting control becomes negative definite when $\xi_\theta > 0$ and $\xi_\psi > 0$.

$$\dot{V} = -s_\theta(1.1\xi_\theta|s_\theta| + \sqrt{\xi_\theta}\sqrt{|s_\theta|}|s_\theta|) - s_\psi(1.1\xi_\psi|s_\psi| + \sqrt{\xi_\psi}\sqrt{|s_\psi|}|s_\psi|). \tag{40}$$

4.4.1. Sensor fault

Sensor fault is sensor drift which affects the system measurements. Thus system equations (9) and (10) becomes,

$$J_\theta\ddot{\theta} = K_{pp}V_{m,p} + K_{py}V_{m,y} - q_\theta + b_1\,, \tag{41}$$

$$J_\psi\ddot{\psi} = K_{yp}V_{m,p} + K_{yy}V_{m,y} - q_\psi + b_2\,, \tag{42}$$

where b_1 and b_2 denotes drift in pitch and yaw encoder. The Lyapunov function for reaching law is

$$\dot{V} = -s_\theta(\xi_\theta|s_\theta| + (b_1/J_\theta)) - s_\psi(\xi_\psi|s_\psi| + (b_2/J_\psi)). \tag{43}$$

For supertwisting control,

$$\begin{aligned}\dot{V} = &-s_\theta\left(1.1\xi_\theta|s_\theta| + \sqrt{\xi_\theta}\sqrt{|s_\theta|}|s_\theta| + (b_1/J_\theta)\right)\\ &- s_\psi\left(1.1\xi_\psi|s_\psi| + \sqrt{\xi_\psi}\sqrt{|s_\psi|}|s_\psi| + (b_2/J_\psi)\right).\end{aligned} \tag{44}$$

Remark 1 *To ensure stability under sensor fault conditions, the values of ξ_θ and ξ_ψ must satisfy $\xi_\theta > |b_1/J_\theta|$ and $\xi_\psi > |b_2/J_\psi|$.*

4.4.2. Actuator fault

Actuator fault is considered as loss of control effectiveness of actuators which is represented as l_k where k denotes the number of actuators. If $l_k = 0$, then there is no fault and $l_k = 1$ denotes complete actuator failure. System with actuator fault is considered as

$$J_\theta\ddot{\theta} = K_{pp}(V_{m,p} - lV_{m,p}) + K_{py}(V_{m,y} - lV_{m,y}) - q_\theta\,, \tag{45}$$

$$J_\psi\ddot{\psi} = K_{yp}(V_{m,p} - lV_{m,p}) + K_{yy}(V_{m,y} - lV_{m,y}) - q_\psi\,. \tag{46}$$

Thus Lyapunov function for reaching law is

$$\dot{V} = -s_\theta(\xi_\theta|s_\theta| - l(s_\theta + (q_\theta/J_\theta)) - s_\psi(\xi_\psi|s_\psi| - l(s_\psi + (q_\psi/J_\psi)). \tag{47}$$

For supertwisting, the Lyapunov function becomes

$$\begin{aligned}\dot{V} = &-s_\theta(1.1\xi_\theta|s_\theta| + \sqrt{\xi_\theta}\sqrt{|s_\theta|}|s_\theta| - l(s_\theta + q_\theta/J_\theta))\\ &- s_\psi(1.1\xi_\psi|s_\psi| + \sqrt{\xi_\psi}\sqrt{|s_\psi|}|s_\psi| - l(s_\psi + q_\psi/J_\psi)).\end{aligned} \tag{48}$$

Remark 2 *To guarantee stability in the event of an actuator fault, the values of ξ_θ and ξ_ψ must satisfy $\xi_\theta > l|q_\theta/J_\theta|$ and $\xi_\psi > l|q_\psi/J_\psi|$.*

4.4.3. Component fault

Change in equivalent viscous damping of pitch and yaw axis is considered as Φ_1 and Φ_2. System with component fault is represented as

$$J_\theta \ddot{\theta} = K_{pp} V_{m,p} + K_{py} V_{m,y} - (B_p + \Phi_1)\dot{\theta} - q_{\theta_1}\,, \tag{49}$$

$$J_\psi \ddot{\psi} = K_{yp} V_{m,p} + K_{yy} V_{m,y} - (B_y + \Phi_2)\dot{\psi} - q_{\psi_1}\,. \tag{50}$$

For reaching law, the Lyapunov function is

$$\dot{V} = -s_\theta(\xi_\theta |s_\theta| - (\Phi_1/J_\theta)\dot{\theta}) - s_\psi(\xi_\psi |s_\psi| - (\Phi_2/J_\psi)\dot{\psi}). \tag{51}$$

For supertwisting control,

$$\begin{aligned}\dot{V} = &-s_\theta \left(1.1\xi_\theta |s_\theta| + \sqrt{\xi_\theta}\sqrt{|s_\theta|}|s_\theta| - (\Phi_1/J_\theta)\dot{\theta}\right) \\ &- s_\psi \left(1.1\xi_\psi |s_\psi| + \sqrt{\xi_\psi}\sqrt{|s_\psi|}|s_\psi| - (\Phi_2/J_\psi)\dot{\psi}\right).\end{aligned} \tag{52}$$

Remark 3 *To ensure stability under component fault conditions, the values of* ξ_θ *and* ξ_ψ *must satisfy* $\xi_\theta > |\Phi_1/J_\theta|$ *and* $\xi_\psi > |\Phi_2/J_\psi|$.

5. Conclusion

In this paper, SMC based on reaching law and super-twisting law is applied to a 2 DOF helicopter as a fault tolerant control strategy. The helicopter system is subjected to various fault conditions in sensors, actuators, and system components which are modeled as additive and multiplicative models. Results shows super-twisting SMC ensures good tracking and control capability with less chattering. Also, the stability of the entire closed-loop system is ensured even in the presence of faults.

References

[1] F. Chen, J. Niu and G. Jiang: Nonlinear fault-tolerant control for hypersonic flight vehicle with multi-sensor faults. *IEEE Access*, **33**(6), (2018), 25427–25436. DOI: 10.1109/ACCESS.2018.2820008.

[2] R. Czyba and L. Stajer: Dynamic Contraction Method approach to digital longitudinal aircraft flight controller design. *Archives of Control Sciences*, **29**(1), (2019), 97–109. DOI: 10.24425/acs.2019.127525.

[3] U. Demirci and F. Kerestecioğlu: Fault tolerant control with re-configuring sliding-mode schemes. *Turkish Journal of Electrical Engineering & Computer Sciences*, **13**(1), (2005), 175–188. DOI: 10.3906/elk-0410-2.

[4] J. Jiang and X. Yu: Fault-tolerant control systems: A comparative study between active and passive approaches. *Annual Reviews in Control*, **36**(1), (2012), 60–72. DOI: 10.1016/j.arcontrol.2012.03.005.

[5] J. Jiang and X. Yu: Robust fault tolerant control with sensor faults for a four-rotor helicopter. *International Journal of Advances in Engineering & Technology*, **3**(1), (2012), 1–13. DOI: 10.1155/2021/6672812.

[6] J. Lan, R.J. Patton and X. Zhu: Integrated fault-tolerant control for a 3-DOF helicopter with actuator faults and saturation. *IET Control Theory & Applications*, **11**(14), (2017), 2232–2241. DOI: 10.1049/iet-cta.2016.1602.

[7] T. Li, Y. Zhang and B.W. Gordon: Passive and active nonlinear fault-tolerant control of a quadrotor unmanned aerial vehicle based on the sliding mode control technique. *Proceedings of the Institution of Mechanical Engineers, Part I: Journal of Systems and Control Engineering*, **227**(1), (2013), 12–23. DOI: 10.1177/0959651812455293.

[8] S. Mallavalli and A. Fekih: A fault tolerant tracking control for a quadrotor UAV subject to simultaneous actuator faults and exogenous disturbances. *International Journal of Control*, **93**(3), (2020), 655–668. DOI: 10.1080/00207179.2018.1484173.

[9] R. Mei: Robust Control for the Suspension Cable System of the Unmanned Helicopter with Sensor Fault under Complex Environment. *Complexity*, (2021). DOI: 10.1155/2021/8869292.

[10] A. Nasiri, S.K. Nguang, A. Swain and A. Akshya: Passive actuator fault tolerant control for a class of MIMO nonlinear systems with uncertainties. *International Journal of Control*, **92**(3), (2019), 693–704. DOI: 10.1080/00207179.2017.1367102.

[11] X. Qi, J. Qi, D. Theilliol, Y. Zhang, J. Han, D. Song and C. Hua: A review on fault diagnosis and fault tolerant control methods for single-rotor aerial vehicles. *Journal of Intelligent & Robotic Systems*, **73**(1), (2014), 535–555. DOI: 10.1007/s10846-013-9954-z.

[12] X. Qi, D. Theilliol, J. Qi, Y. Zhang, J. Han, D. Song, L. Wang and Y. Xia: Fault diagnosis and fault tolerant control methods for manned and unmanned helicopters: a literature review. *2013 Conference on Control and Fault-Tolerant Systems (SysTol)*, (2013), 132–139. DOI: 10.1109/SysTol.2013.6693906.

[13] L. Qin, X. He, R. Yan and D. Zhou: Active fault-tolerant control for a quadrotor with sensor faults. *Journal of Intelligent & Robotic Systems*, **88**(2), (2017), 449–467. DOI: 10.1007/s10846-017-0474-0.

[14] Y. Qiwei and Y. Rui: Nonsingular terminal sliding mode based passive fault-tolerant control of a 3-DOF helicopter system. *IFAC-PapersOnLine*, **51**(24), (2018), 1368–1372. DOI: 10.1016/j.ifacol.2018.09.556.

[15] R. Singh and B. Bhushan: A novel fault classification-based fault-tolerant control for two degree of freedom helicopter systems. *International Journal of Adaptive Control and Signal Processing*, **34**(8), (2020), 1080–1104. DOI: 10.1002/acs.3121.

[16] J. Tan, Y. Fan, P. Yan, C. Wang and H. Feng: Sliding mode fault tolerant control for unmanned aerial vehicle with sensor and actuator faults. *Sensors*, **19**(3), (2019), 643. DOI: 10.3390/s19030643.

[17] I. Ullah and H. L. Pei: Sliding mode tracking control for unmanned helicopter using extended disturbance observer. *Archives of Control Sciences*, **29**(1), (2019), 169–199. DOI: 10.24425/acs.2019.127530.

[18] B. Wang and Y. Zhang: An adaptive fault-tolerant sliding mode control allocation scheme for multirotor helicopter subject to simultaneous actuator faults. *IEEE Transactions on Industrial Electronics*, **65**(5), (2017), 4227-4236. DOI: 10.1109/TIE.2017.2772153.

[19] X. Yu and J. Jiang: A survey of fault-tolerant controllers based on safety-related issues. *Annual Reviews in Control*, **39**, (2015), 46–57. DOI: 10.1016/j.arcontrol.2015.03.004.

[20] Y. Zhang, A. Chamseddine, C.A. Rabbath, B. W. Gordon, C-Y Su, S. Rakheja, C. Fulford, J. Apkarian and P. Gosselin: Development of advanced FDD and FTC techniques with application to an unmanned quadrotor helicopter testbed. *Journal of the Franklin Institute*, **350**(9), (2013), 2396–2422. DOI: 10.1016/j.jfranklin.2013.01.009.

[21] Y. Zhang and J. Jiang: Bibliographical review on reconfigurable fault-tolerant control systems. *Annual Reviews in Control*, **32**(2), (2008), 229–252. DOI: 10.1016/j.arcontrol.2008.03.008.